가열된 동축류내 층류 메탄/수소 부상화염의 안정화 과정에 관한 수치해석적 연구

정기성*. 김승욱*. 정석호**. 유춘상*†

A numerical study of the stabilization mechanism of an autoignited laminar methane/hydrogen lifted jet flame in heated coflow

Ki Sung Jung*, Seung Ook Kim*, Suk Ho Chung**, Chun Sang Yoo*†

ABSTRACT

A temporal evolution of methane/hydrogen mixtures in the laminar heated coflow jet is numerically simulated using laminarSMOKE with 30-species skeletal methane/air kinetic mechanism. The result shows that an ignition kernel first develops at the far downstream of the final stabilization location, and it propagates upstream until the overall flame structure exhibits the stationary lifted flame. From the calculation of displacement speed of flamebase at each different time, it is verified that an autoignition is dominant during the early stage of flame development right after the ignition kernel generation, and the flame propagation becomes dominant when the lifted flame is stabilized by balancing with the local flow velocity. In addition, the 1-D laminar flame speed calculation with various upstream temperature conditions supports that flame propagation is a key stabilization mechanism in lifted flame by showing that density weighted displacement speed of flamebase at steady state is within the range of the calculated 1-D laminar flame speed.

Key Words : Lifted flame, autoignition, flame stabilization, tribrachial flame

Many types of researches on autoignited laminar lifted flame have been carried out recently, but the understanding of the stabilization mechanism of autoignited lifted jet flame is relatively limited. From our previous research, stabilization mechanism of laminar autoignited methane/hydrogen lifted flame was studied by applying species transport budget analysis and Chemical Explosive Mode Analysis (CEMA) of the steady-state solution, suggesting that autoignition plays a critical role in the stabilization of laminar lifted flames. According to a previous study of the temporal evolution of autoignited C_2H_4 jet flame with the addition of ozone [1], however, it was observed that ignition kernel is first generated at the far downstream of stabilization point, and it seems to propagate toward the upstream with the speed of more than 10 times of laminar flame speed, S_L. A similar observation has been reported in previous numerical simulations [2,3]. These experimental and numerical results imply that flame stabilization of autoignited lifted flame does not depend solely on the autoignition, but rather flame propagation would be important for stabilizing lifted flames. Thus, detailed research on the transient behavior of autoignition kernel development is required for the comprehensive understanding of the stabilization mechanism of autoignited lifted flame.

In the present study, therefore, a temporal evolution of autoignited laminar lifted methane/hydrogen flame is numerically simulated using laminarSMOKE [4,5], which is an open-source code based on OpenFOAM [6]. Skeletal kinetic mechanism of 30 species with 184 elementary reactions [7] based on GRI-

* 울산과학기술원 기계공학과
** KAUST Clean Combustion Research Center
† 연락저자, csyoo@unist.ac.kr
TEL : (052)217-2322 FAX : (052)217-2409

Mech 3.0 is adopted for the simulation. The main domain size is 6.65 cm × 50 cm in the radial, $r-$, and the axial, $z-$ directions. The diameter of fuel jet nozzle is 1.88 mm with 0.5 mm nozzle thickness, and 3 cm of fuel nozzle is attached to the main domain, which protrudes 1 cm above the coflow air inlet. In the $r-$ directions, a grid space of 0.1 mm is uniformly applied for $0 \leq r \leq 1$ cm and the stretched grids are distributed to the remaining domain. In the $z-$directions, 0.1 mm grids are equally applied.

All the boundary conditions are consistent with the experimental conditions. Fuel mole fraction in fuel jet inlet, X_F, is 0.2, and hydrogen ratio of fuel, R_H, is 0.3. Fully developed pipe flow condition is applied to the fuel jet inlet with the mean velocity of U_0 = 25 m/s, which represents the lifted flame with tribrachial edge, and coflow velocity, U_c, is fixed to be 1.1 m/s. Inlet temperature condition, T_0, is 950 K. Zero-gradient and atmospheric pressure conditions are applied in inlet and outlet, respectively. All the other outlet boundary conditions are zero-gradient.

Figure 1 shows the temperature and H_2O_2 species isocontours of the lifted flame with tribrachial edge (U_0 = 25 m/s) at several different times. At t = 0.120 s, an autoignition ignition kernel develops at 11.8 cm downstream of the final stabilized point, and the flamebase subsequently moves to the upstream until the overall flame structure exhibits the stationary lifted flame having the liftoff height, H_L. Here, flamebase is defined as the most upstream point of Y_{OH} = 2 × 10^{-4} isoline, which is approximately 5% of the maximum OH mass fraction value of the entire domain.

Several points are noted from the Fig. 1. First, overall flame structure moves to the upstream with significantly fast speed from 0.120 to 0.123 s, while the flame moves to the final stabilized location with relatively low speed from 0.138 s to the steady state. Therefore, it is conjectured that autoignition plays a key role in increasing the flame speed during the early stage of flame development after the ignition kernel forms, and flame propagation would become dominant as flamebase moves to the stabilization point. Second, at t = 0.120 s, temperature already starts to increase at the upstream of ignition kernel generation, which is attributed to the thermal runaway step of autoignition process. It proposes that flame propagation speed toward the upstream is not a constant value but would be exponentially proportional to the upstream temperature because laminar flame speed S_L is known as a function of reaction rate, ω: $S_L \sim \sqrt{\omega} \sim \exp(-T_a/2T)$. It is also noted that the presence of intermediate species such as CH_2O, HO_2, and H_2O_2 are predominant at the upstream of ignition kernel generation, which implies that the effect of autoignition would be important upstream of the flame region.

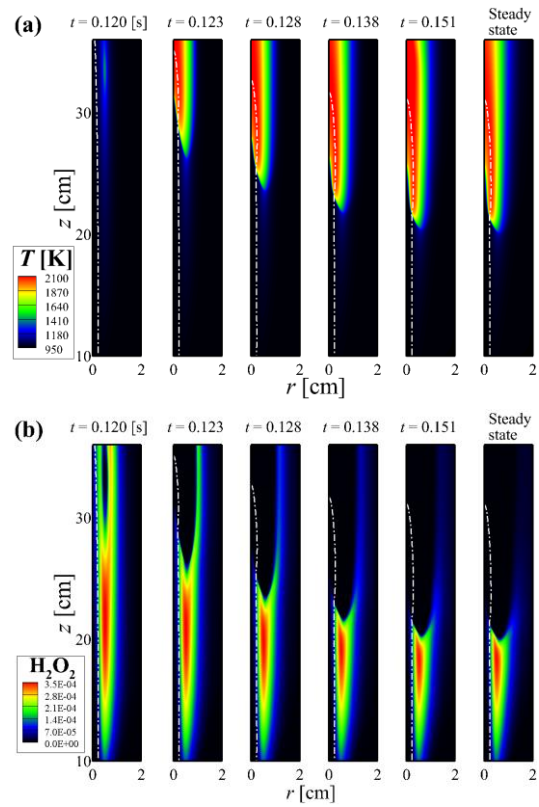

Fig. 1 Temperature (a) and mass fraction of H_2O_2 (b) isocontours of temporal evolution of laminar lifted flame with tribrachial edge (U_0 = 25 m/s). White dash-dotted line represents the stoichiometric mixture fraction isoline, ξ_{st} (=0.368)

Based on the observation in Fig. 1, the stabilization mechanism of the lifted flame with tribrachial edge is schematically illustrated in Figs. 2a and b. First, the upstream temperature

gradually increases with the increasing z due to the thermal runaway process as shown in Fig 2a, and a detectable ignition kernel is generated at the far downstream (red circle in Figs. 2a and 2b). Second, the generated ignition kernel contains high convective energy, it therefore forces the flamebase to move back to the upstream with high front speed, S_{ig}, which is delineated in the red line in Fig. 2b. Here, S_{ig} is related to the ignition delay time, τ_{ig} : $S_{ig} = 1/|\nabla\tau_{ig}|$ [8], and it is also a function of temperature as follows.

$$S_{ig} = |\nabla\tau_{ig}|^{-1} \sim (|\nabla\exp(T_a/T)|)^{-1} \sim \exp(-T_a/T)$$

Third, the autoignited lifted flame would lose its autoignition characteristics with the temporal change, and the overall flame speed characteristics during the temporal evolution would be converted to the normal flame propagation, which has on a scale of laminar flame speed S_L (blue line in Fig. 2b). Finally, the propagating flame is stabilized at the location where the propagation speed balances the local flow normal velocity, U_N. Here, U_N is regarded as a constant over the axial location, z because it's variation would be negligible compared to S_{ig} and S_L, which depend exponentially on the upstream temperature, T.

To validate the proposed stabilization mechanism of laminar lifted flame with tribrachial edge, flame propagation speed of the flamebase is calculated at each different time by adopting displacement speed, S_d [9-11],

$$S_d = \frac{1}{\rho|\nabla Y_k|}\left(\dot{\omega}_k - \frac{\partial}{\partial x_j}(\rho Y_k V_{j,k})\right)$$

where Y_k is the species mass fraction, ρ the mixture density, $\dot{\omega}_k$ the net production rate of species k, $V_{j,k}$ the species diffusion velocity in the direction j. Figure 3 shows the S_d and U_N at the flamebase with the different time of U_0 = 25 m/s case. It is readily observed that S_d is at its peak (S_d = 44.4 m/s) when the ignition kernel first develops, and S_d decreases drastically during t = 0.12 ~ 0.13 s. After t = 0.13 s, the variation of S_d on time is marginally observed, which is qualitatively similar to the schematic drawing of Fig. 2b. Therefore, it implies that autoignition, which front speed is much faster than the laminar flame speed, is dominantly affecting during the early stage of ignition kernel generation, and the flame propagation become dominant as flamebase moves to the upstream. It is also noted that local flow normal velocity at the flamebase, U_N, is almost constant as compared to S_d, which is consistent with the schematic drawing of Fig. 2b. Additionally, S_d at the steady state is balanced with U_N, verifying that the main stabilization mechanism of autoignited stationary lifted flame is a flame propagation, which flame propagating speed is balanced with the local flow velocity.

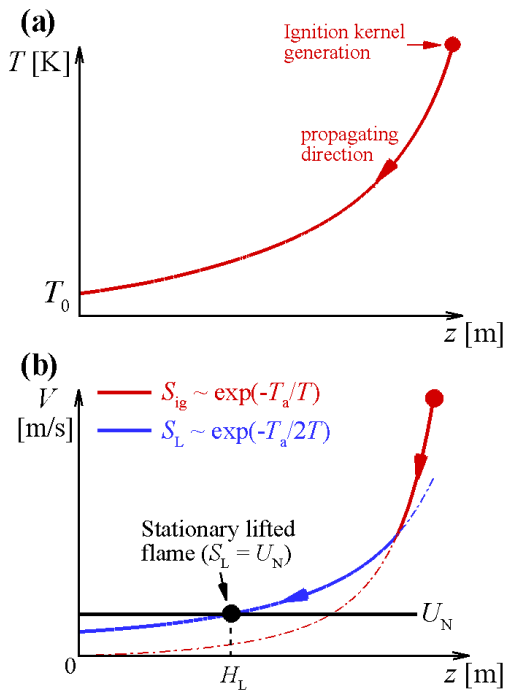

Fig. 2 Schematic drawings of temperature profile (a), and stabilization of laminar lifted flame (b).

To make sure the stabilization mechanism of the present case, 1-D laminar flame speed, S_L, is calculated for various initial conditions. It is generally known that density weighted displacement speed, S_d^*, has a similar value with S_L under the normal flame propagation situations [9-11]. In the present jet

configuration, however, it is hard to examine the precise reference S_L because the flame propagates to non-uniform upstream temperatures.

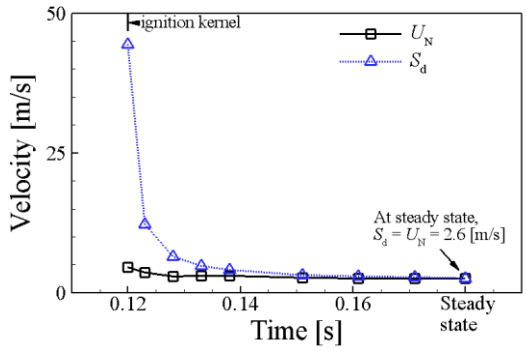

Fig. 3 Displacement speed S_d and local flow normal velocity U_N as a function of time.

Therefore, we calculate S_L in 1-D domain with varying the initial temperature from 950 K (inlet temperature) to 1080, 1100, and 1150 K (5, 3, 1 mm upstream of flamebase, respectively), and check whether S_d^* at the steady state is within the range of the calculated S_L or not. Here, temperature at each different upstream distance is obtained by following the mixture fraction isoline passing through the flamebase. The original unburned species components at the inlet (i.e., CH_4, H_2, O_2, and N_2) are estimated from the species concentrations at the flamebase by using the element conservation law, and the estimated unburned species are adopted as an initial species condition in the S_L calculation. The obtained S_L with various temperature conditions are summarized in the table 1.

Note that density weighted displacement speed S_d^* is 2 m/s at the steady state, which is within the range of S_L at 1 ~ 3 mm upstream of flamebase ($S_{L,T=1100K} < S_d^* < S_{L,T=1150K}$). Therefore, a similar value of S_d^* compared to S_L implies that flame propagation is the dominant stabilization mechanism in lifted flame.

Table 1 Calculated S_L with various T

T description	T [K]	S_L [m/s]
Inlet temperature (T_0)	950	0.3
5 mm upstream of flamebase	1080	1.3
3 mm upstream of flamebase	1100	1.6
1 mm upstream of flamebase	1150	2.3

후 기

This research was supported by Basic Science Research Program through the National Research Foundation of Korea (NRF) funded by the Ministry of Science, ICT & Future Planning (NRF-2015R1A2A2A01007378).

참고 문헌

[1] X. Gao, J. Zhai, W. Sun, T. Ombrello, C. Carter, 53rd AIAA/SAE/ASEE Joint Propulsion Conference, 2017, 4774.
[2] S. K. Choi, S. Al-Noman, S. H. Chung, Combust. Sci. Technol., 187, 2015, pp 132 – 147.
[3] S. Al-Noman, S. K. Choi, S. H. Chung, Combust. Flame, 171, 2016, pp 119 – 132.
[4] A. Cuoci, A. Frassoldati, T. Faravelli, E. Ranzi, Combust. Flame, 160, 2013, pp 870 – 886.
[5] A. Cuoci, A. Frassoldati, T. Faravelli, E. Ranzi, Energy. Fuels, 27, 2013, pp 7730-7753
[6] H. G. Weller, G. Tabor, H. Jasak, C. Fureby, Comput. Phys. 12, 1998, pp. 620-631.
[7] T. F. Lu, C. K. Law, Combust. Flame, 154, 2008, pp. 761-774.
[8] Y. B. Zeldovich, Combust. Flame, 39, 1980, pp. 211-214.
[9] J. H. Chen, E. R. Hawkes, R. Sankaran, S. D. Mason, H. G. Im, Combust. Flame, 160, 2013, pp 870 – 886.
[10] M. B. Luong, Z. Luo, T. Lu, S. H. Chung, C. S. Yoo, Combust. Flame 160, 2013, pp 2038 – 2047.
[11] H. G. Im, J. H. Chen, Combust. Flame 119, 1999, pp 436 – 454.